FULL PAPER

Dalton
www.rsc.org/dalton

# Syntheses, structural analyses and redox kinetics of four-coordinate $[CuL_2]^{2+}$ and five-coordinate $[CuL_2(solvent)]^{2+}$ complexes (L = 6,6′-dimethyl-2,2′-bipyridine or 2,9-dimethyl-1,10-phenanthroline): completely gated reduction reaction of $[Cu(dmp)_2]^{2+}$ in nitromethane†

**Sumitaka Itoh,[a] Nobuyuki Kishikawa,[a] Takayoshi Suzuki[b] and Hideo D. Takagi*[c]**

[a] *Department of Chemistry, Graduate School of Science, Nagoya University, Furo-cho, Chikusa, Nagoya, 464-8602, Japan*

[b] *Department of Chemistry, Graduate School of Science, Osaka University, Toyonaka, Osaka, 560-0043, Japan*

[c] *Inorganic Chemistry Division, Research Center for Materials Science, Nagoya University, Furo-cho, Chikusa, Nagoya, 464-8602, Japan. E-mail: h.d.takagi@nagoya-u.jp*

***Received 28th September 2004, Accepted 2nd February 2005***
***First published as an Advance Article on the web 16th February 2005***

$[Cu(2,9\text{-dimethyl-1,10-phenanthroline})_2]^{2+}$ and $[Cu(6,6'\text{-dimethyl-2,2'-bipyridine})_2]^{2+/+}$ complexes with no coordinated solvent molecule were synthesized and the crystal structures were analyzed: the coordination geometry around the Cu(I) center was in the $D_{2d}$ symmetry while a $D_2$ structure was observed for the four-coordinate Cu(II) complexes. Coordination of a water or an acetonitrile molecule was found in the trigonal plane of the five-coordinate Cu(II) complex in the *Tbp* (trigonal bipyramidal) structure. Spectrophotometric analyses revealed that the $D_2$ structure of the Cu(II) complex was retained in nitromethane, although a five-coordinate *Tbp* species (green in color), was readily formed upon dissolution of the solid (reddish brown) in acetonitrile. The electron self-exchange reaction between $D_{2d}$-Cu(I) and $D_2$-Cu(II), observed by the NMR method, was very rapid with $k_{ex} = (1.1 \pm 0.2) \times 10^5$ kg mol$^{-1}$ s$^{-1}$ at 25 °C ($\Delta H^* = 15.6 \pm 1.3$ kJ mol$^{-1}$ and $\Delta S^* = -96 \pm 4$ J mol$^{-1}$ K$^{-1}$), which was more than 10 times larger than that reported for the self-exchange reaction between $D_{2d}$-Cu(I) and *Tbp*-Cu(II) in acetonitrile. The cross reduction reactions of $D_2$-Cu(II) by ferrocene and decamethylferrocene in nitromethane exhibited a completely gated behavior, while the oxidation reaction of $D_{2d}$-Cu(I) by $[Ni(1,4,7\text{-triazacyclononane})_2]^{3+}$ in nitromethane estimated an identically large self-exchange rate constant to that directly obtained by the NMR method. The electron self-exchange rate constant estimated from the oxidation cross reaction in 50% v/v acetonitrile–nitromethane mixture was 10 times smaller than that observed in pure nitromethane. On the basis of the Principle of the Least Motion (PLM) and the Symmetry Rules, it was concluded that gated behaviors observed for the reduction reactions of the five-coordinate Cu(II)–polypyridine complexes are related to the high-energy $C_{2v} \rightarrow D_{2d}$ conformational change around Cu(II), and that the electron self-exchange reactions of the Cu(II)/(I) couples are always adiabatic through the $C_{2v}$ structures for both Cu(II) and Cu(I) since the conformational changes between $D_{2d}$, $D_2$ and $C_{2v}$ structures for Cu(I) as well as the conformational change between *Tbp* and $C_{2v}$ structures for Cu(II) are symmetry-allowed. The completely gated behavior observed for the reduction reactions of $D_2$-Cu(II) species in nitromethane was attributed to the very slow conformational change from the ground-state $D_2$ to the entatic $D_{2d}$ structure that is symmetry-forbidden for d$^9$ metal complexes: the very slow back reaction, the forbidden conformational change from entatic $D_{2d}$ to the ground-state $D_2$ structure, ensures that the rate of the reduction reaction is independent of the concentration of the reducing reagent.

## Introduction

Electron transfer reactions involving Cu(II)/(I) centers have attracted attentions of many researchers since these reactions are strongly related to the biologically important catalytic processes.[1,2] Copper enzymes, especially that exhibit strong blue color, possess $N_2S_2$ coordination environment around the Cu(II) ion and the electron transfer (ET) reactions at these copper sites are extremely rapid compared with those involving ordinary Cu(II) complexes with the tetragonally distorted octahedral coordination environment.[3]

It has not been long since the gated phenomenon, in which the electron self-exchange rate constants estimated from the cross reactions of oxidation and reduction directions are significantly different from each other,[4–6] was recognized for the first time (Appendix A). The initial explanation by Lee and Anson, that the correct self-exchange rate constant for such reactions should be expressed by the geometric mean of the rate constants estimated from oxidation and reduction cross reactions,[7] was shown to be invalid by the later investigations.

Among investigations carried out to date, intensive and systematic studies by Rorabacher and co-workers seem to have largely improved understandings of the gated phenomena: they examined ET reactions of Cu(II)/(I)–macrocyclic polythioether

---

† Electronic supplementary information (ESI) available: Table S1: Redox potentials. Table S2: Dependence of the line width of the methyl proton signal on the concentration of $[Cu(dmp)_2]^{2+}$ in nitromethane at various temperatures. Table S3: Dependence of the rate constant on the concentration of $[Ni(tacn)_2]^{3+}$ for the electron transfer reaction between $[Cu(dmp)_2]^{+}$ and $[Ni(tacn)_2]^{3+}$. Table S4: Dependence of the rate constant for the reduction reaction of $[Cu(dmp)_2]^{2+}$ by ferrocene on the concentration of ferrocene in nitromethane at various temperatures. Table S5: Temperature dependence of the rate constant for the conformational change of four-coordinate $[Cu(dmp)_2]^{2+}$ from the $D_2$ to $D_{2d}$ structure in nitromethane. Table S6: Dependence of the rate constant on the concentration of $[Cu(dmbp)_2]^{2+}$ for the electron transfer reaction between $[Cu(dmp)_2]^{+}$ and $[Cu(dmbp)_2]^{2+}$. See http://www.rsc.org/suppdata/dt/b4/b415057k/

DOI: 10.1039/b415057k

complexes and found that the coordination structural change takes place essentially at the Cu(I) site while the coordination geometry around the Cu(II) species is not largely altered.[8–12] They related this phenomenon to the biologically important catalytic processes and postulated a dual-pathway Square Scheme described in Scheme 1. Rorabacher recently reviewed ET reactions by Cu(II)/(I) centers,[13] in which he seems to have confirmed that the gated ET reactions exhibited by copper complexes are successfully explained by this scheme.[8–12] In general, ET reactions of Cu(II)/(I)–polythioether complexes proceed through path A in Scheme 1, and the direction in which the estimated self-exchange rate constant is much smaller than that directly measured by NMR is gated: *i.e.* the self-exchange rate constant estimated from the non-gated direction is almost identical to that measured directly by the NMR method. Rorabacher and co-workers attributed the origin/reason of the gated phenomena essentially to the sluggish conformational change of the coordinated multidentate macrocyclic ligands:[8–12] the ground-state geometries of Cu(I) and Cu(II) species should come close to each other at the transition state for the electron transfer reaction, according to the Marcus theory for the outer-sphere ET reactions.[14–16]

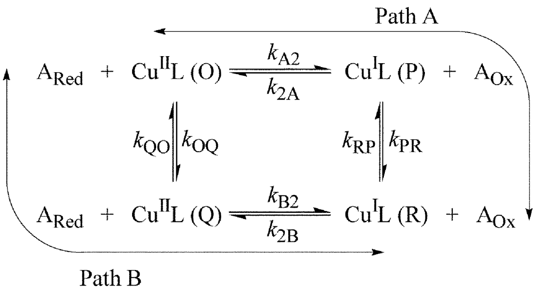

**Scheme 1** Square Scheme postulated by Rorabacher *et al.*

We examined redox reactions of various Cu(II)/(I)–polypyridine complexes and found that there are cases where Rorabacher's Square Scheme may not apply:[17–19] (1) the electron self-exchange rate constants estimated from both reduction and oxidation directions were very small in the case of the $[Cu(dmbp)_2]^{2+/+}$ couple (dmbp = 6,6′-dimethyl-2,2′-bipyridine) when the counter reagent was $[Ru(hfac)_3]^{0/-}$ (hfac = hexafluoroacetylacetonate, see Appendix B), while the directly measured electron self-exchange rate constant for the $[Cu(dmbp)_2]^{2+/+}$ couple exhibited an ordinarily large value, and (2) most of the polypyridine ligands used in our studies are didentate and no sluggish conformational change in the coordinated ligands is expected for the alterations of the coordination geometries around Cu(II) and Cu(I) centers. In addition, the results of the original study concerning the volume analyses of the electron self-exchange reaction for the $[Cu(dmp)_2]^{2+/+}$ couple (2,9-dimethyl-1,10-phenanthroline) strongly indicate that the electron self-exchange reactions between the five-coordinate Cu(II) and four-coordinate Cu(I) complexes are adiabatic.[20] Therefore, we started to consider that the Square Scheme (Scheme 1), although it appears to successfully explain some of the observed gated phenomena, does not describe the exact nature of the gated behavior. We recently postulated a possible origin of the gated phenomena on the basis of the physico-chemical consideration of the electron transfer reactions,[19,21] although we have to admit that a few of our previous spectrochemical analyses on the basis of the method by Yokoi and Addison[22] are invalid:[23] since cross reactions, especially with other metal complexes, of Cu species without low-energy CT bands are slow, uneven structural changes in the gated electron transfer reactions that involve large structural changes before the ET process are important to achieve sufficient electronic coupling between the reactants so as to provide a low-energy CT-perturbed reaction pathway. Although this mechanism seems to explain most of the reported gated phenomena, it certainly needs further evidence and explanations to justify the theory (Appendix C).

In this study, we report two different crystal structures for the $[Cu(dmp)_2]^{2+}$ complex: one of which with coordinated water or acetonitrile is light green in color while the four-coordinate complex with no coordinated solvent molecule exhibited reddish color in the solid and in nitromethane. It was found that the cross reaction between Cu(I) and Cu(II) complexes each bearing different didentate ligands is rapid and certainly not gated in acetonitrile although the ground-state structures of these Cu(I) and Cu(II) complexes are significantly different (it has been already reported that the reduction cross reactions of these two copper complexes with other metals are gated in acetonitrile).[17,18] The very different redox behaviors exhibited by four- and five-coordinate Cu(II) complexes were explained on the basis of the Symmetry Rules and the Principle of the Least Motion.[24–26]

## Experimental

### Materials

Nitromethane, obtained from Wako Pure Chemicals Inc., was dried over molecular sieves 4A, followed by distillation under reduced pressure. Acetonitrile was obtained from Wako, and purified by distillation from phosphorus pentoxide. The content of the residual water in thus purified nitromethane and acetonitrile was examined by a Mitsubishi Chemical CA07 Karl-Fisher apparatus, by which the amount of residual water was determined to be less than 1 mmol $kg^{-1}$. Tetra-*n*-butylammonium perchlorate (TBAP) was twice recrystallized from the mixture of ethyl acetate–pentane solution, and dried under reduced pressure. Ferrocene (Wako) was purified by sublimation. All other chemicals used especially for the synthesis of metal complexes were purchased from Wako, Aldrich, and TCI, and were used without further purification. Bis(2,9-dimethyl-1,10-phenanthroline)- and bis(6,6′-dimethyl-2,2′-bipyridine)-copper(II) and -(I) perchlorate were synthesized by reported methods.[20] Anal. Calc. for $[Cu(dmp)_2](ClO_4)_2$ = $CuC_{28}H_{24}N_4Cl_2O_8$: C, 49.5; N, 8.25; H, 3.56. Found: C, 50.5; N, 8.16; H, 3.65. Anal. Calc. for $[Cu(dmp)_2]ClO_4$ = $CuC_{28}H_{24}N_4ClO_4$: C, 58.0; N, 9.67; H, 4.17. Found: C; 58.6, N, 9.87; H, 4.10. Anal. Calc. for $[Cu(dmbp)_2(H_2O)](ClO_4)_2$ = $CuC_{24}H_{26}N_4Cl_2O_9$: C, 44.4; H, 4.04; N, 8.63. Found: C, 44.8; H, 4.03; N, 8.72. Anal. Calc. for $[Cu(dmbp)_2]ClO_4$ = $CuC_{24}H_{24}N_4ClO_4$: C, 54.2; H, 10.5; N, 4.55. Found: C, 54.4; H, 9.98; N, 4.60. $[Ni(tacn)_2](ClO_4)_3$[27] was synthesized by the literature method. Anal. Calc. for $NiC_{12}H_{30}N_6Cl_3O_{12}$: C, 23.42; H, 4.91; N, 13.66. Found: C, 23.42; H, 4.96; N, 13.55% (**CAUTION!** *Perchlorate salts of metal complexes with organic ligands are potentially explosive.*)

### X-Ray crystal structures

Single crystals of $[Cu(dmp)_2](ClO_4)_2\cdot 2CH_3NO_2$ and $[Cu(dmbp)_2](ClO_4)_2$ were obtained from recrystallization with nitromethane–diethyl ether, and a single crystal of $[Cu(dmbp)_2]ClO_4$ was obtained from recrystallization with acetonitrile–diethyl ether, while $[Cu(dmbp)_2(H_2O)](ClO_4)_2$ was crystallized from acetonitrile–water solution. Each crystal suitable for the X-ray diffraction study was mounted with a cryoloop and flash-cooled by the cold nitrogen stream.

The X-ray intensities were measured on a Rigaku imaging plate area detector Raxis-rapid [−73(2) °C, graphite-monochromated Mo-Kα radiation ($\lambda$ = 0.71073 Å), the oscillation scan mode, $2\theta < 55°$, 100 × 100 pixel mode]. The structures were solved by the direct method using SIR92 program,[28] and refined on $F^2$ (with all independent reflections) using the SHELXL97 program.[29] All non-hydrogen atoms were refined anisotropically, and H atoms were introduced theoretically and treated by riding models. All calculations were carried out using

**Table 1** Crystallographic data

| Compound | $[Cu(dmp)_2](ClO_4)_2\cdot 2CH_3NO_2$ | $[Cu(dmbp)_2](ClO_4)_2$ | $[Cu(dmbp)_2(H_2O)](ClO_4)_2$ | $[Cu(dmbp)_2]ClO_4$ |
|---|---|---|---|---|
| Formula | $C_{30}H_{30}Cl_2CuN_6O_{12}$ | $C_{24}H_{24}Cl_2CuN_4O_8$ | $C_{24}H_{26}Cl_2CuN_4O_9$ | $C_{24}H_{24}ClCuN_4O_4$ |
| FW | 801.04 | 630.91 | 648.93 | 531.46 |
| $T$/K | 200(2) | 200(2) | 200(2) | 200(2) |
| Color, shape | Red brown, prism | Dark red, columnar | Green, plate | Red, prism |
| Crystal dimensions/mm | 0.18 × 0.16 × 0.12 | 0.32 × 0.20 × 0.18 | 0.22 × 0.22 × 0.14 | 0.28 × 0.18 × 0.12 |
| Crystal system | Triclinic | Triclinic | Monoclinic | Monoclinic |
| Space group, $Z$ | $P\bar{1}$, 2 | $P\bar{1}$, 4 | $P2_1/a$, 4 | $P2_1/a$, 4 |
| $a$/Å | 8.456(4) | 9.939(8) | 14.008(6) | 8.833(5) |
| $b$/Å | 13.476(5) | 14.511(11) | 10.951(5) | 21.684(12) |
| $c$/Å | 14.730(6) | 19.074(17) | 18.099(5) | 12.384(7) |
| $\alpha$/° | 102.72(3) | 74.06(8) | 90 | 90 |
| $\beta$/° | 91.32(3) | 86.30(7) | 101.57(3) | 95.68(4) |
| $\gamma$/° | 92.46(3) | 78.02(7) | 90 | 90 |
| $V$/Å$^3$ | 1635.0(11) | 2587(4) | 2720.0(18) | 2361(2) |
| $D_c$/Mg m$^{-3}$ | 1.627 | 1.620 | 1.585 | 1.495 |
| $F$(000) | 822 | 1292 | 1332 | 1096 |
| $\mu$(Mo-K$\alpha$)/mm$^{-1}$ | 0.906 | 1.108 | 1.061 | 1.077 |
| Reflns./param. ratio | 7210/460 | 10610/703 | 5915/361 | 5403/308 |
| $R1$ $[F_o^2 > 2\sigma(F_o^2)]$ | 0.057 | 0.040 | 0.057 | 0.061 |
| $wR2$ (all reflns.) | 0.169 | 0.106 | 0.139 | 0.104 |
| GoF | 1.000 | 1.043 | 1.015 | 1.001 |

a teXsan software package.[30] Crystallographic data are collected in Table 1.

CCDC reference numbers 251495–251498.

See http://www.rsc.org/suppdata/dt/b4/b415057k/ for crystallographic data in CIF or other electronic format.

### Kinetic and electrochemical measurements (Appendix D)

All manipulations were carried out in an atmosphere of dry argon to avoid any possible contamination by water and oxygen from the environment. Kinetic measurements were carried out by a Unisoku RA401 stopped-flow apparatus. The reactions were monitored by observation of the absorbance change at 456 nm (the absorption maximum of $[Cu(dmp)_2]^+$).

Electrochemical measurements were carried out by using a BAS 100 B/W Electrochemical Analyzer with a standard three-electrode configuration: a 1.6 mmϕ platinum disk was used as the working electrode, a platinum wire as the counter electrode, and a $Ag/AgNO_3$ electrode in 0.1 M solution of TBAP in acetonitrile was used as the reference electrode. The redox potentials of complexes are reported with reference to that for the ferricenium–ferrocene couple in the same solvent (Table S1, ESI†). The NMR measurements were carried out by a Bruker AMX-400WB spectrometer.

## Results

### X-Ray crystal structures

**$[Cu(dmbp)_2]ClO_4$.** The coordination geometry around the copper center was revealed to have a distorted tetrahedral geometry (Fig. 1(a)). The dihedral angle between the planes defined by the copper center and each set of the bipyridine nitrogen atoms is 80.7° and is compared with that (80.9°) reported for $[Cu(dmbp)_2]BF_4$.[31] These dihedral angles are slightly smaller than that expected for the regular $D_{2d}$ geometry and consistent with those for the other Cu(I)–2,2′-bipyridine complexes.[32,33] Such small distortions have been believed to be caused by the crystal packing forces, and the structures of these species in solution are believed to be in the regular $D_{2d}$ geometry: although the tetrahedral Cu(II) complexes suffer from the first-order Jahn–Teller distortion to produce species in the $D_{2d}$ symmetry, there is no reason to rationalize such a distortion for Cu(I) complexes.[34–36] However, the symmetry arguments (see Discussion) conclude that four-coordinate Cu(I) complexes with the $d^{10}$ electronic configuration are fluxional among the $C_{2v}$, $D_{2d}$ and $D_2$ structures when they exhibit low-energy MLCT bands.

It seems that the factor which governs the N–Cu–N angle is the bite angles of the didentate dmbp and dmp ligands. The range of the Cu–N bond distances, 2.021(2)–2.047(2) Å, lies within the range of those previously found for the Cu(I) complexes with 2,2′-bipyridine ligands. Selected bond lengths and angles are listed in Table 2. The dmbp ligands are nonplanar and slightly twisted around the 2,2′-carbon-carbon bond (2.9(1) for N1 and N2 and 13.3(1)° for N3 and N4). These distortions are also consistent with those reported for $[Cu(dmbp)_2]BF_4$ and $[Cu(2,2'\text{-bipyridine})_2]^+$ complexes.[31–33]

**$[Cu(dmp)_2](ClO_4)_2\cdot 2CH_3NO_2$ and $[Cu(dmbp)_2](ClO_4)_2$.** The crystals of these complexes were obtained by recrystallization from nitromethane–diethyl ether mixture, although $[Cu(dmp)_2](ClO_4)_2\cdot 2CH_3NO_2$ decomposed immediately by exposing the crystal to the air. The X-ray crystal structures (Fig. 1(b) and (c) and Table 2) revealed that these complexes have $D_2$ coordination geometries around the Cu(II) center. These include the first example of four-coordinate copper(II) complex bearing 1,10-phenanthroline type ligand.[37] The Cu–O(perchlorate anion) distance (2.485(4) Å) in $[Cu(dmp)_2]^{2+}$ is appreciably shorter than that in the crystal of $[Cu(dmbp)_2]^{2+}$ (2.984(3) for mol1 and 3.014(3) Å for mol2), while other bond distances are identical to each other in these two complexes. Therefore, there is no significant interaction between the copper(II) center and the perchlorate oxygen, and the relatively short Cu–O distance is attributed to the crystal packing effect. The dihedral angles between the planes defined by the copper center and each set of the phenanthroline or bipyridine nitrogen atoms are 60.34° in $[Cu(dmp)_2]^{2+}$, and 61.40° (mol1) and 62.78° (mol2) in $[Cu(dmbp)_2]^{2+}$. These dihedral angles are significantly smaller than the right angle, and therefore these complexes are clearly in the $D_2$ symmetry. The $D_2$ structures in these complexes are not the result of the Jahn–Teller effect for the complexes in the $D_{2d}$ symmetry, since no low-energy $B_1$ vibration mode is active for $d^9$ Cu(II) in this symmetry. Therefore, the ground-state structures of these four-coordinate Cu(II) complexes are $D_2$ as a result of the steric repulsion between the bulky methyl groups on the ligands, otherwise these complexes are expected to have square-based structure: the dihedral angle reported for the four-coordinate $[Cu(bipy)_2]^{2+}$ complex is only 44.6°.[37] Such a conclusion was verified by the MM calculations (Appendix E).

**$[Cu(dmbp)_2(H_2O)](ClO_4)_2$.** The crystal structure of $[Cu(dmbp)_2(H_2O)](ClO_4)_2$ (Fig. 1(d)) is similar to the one for previously reported $[Cu(dmp)_2(H_2O)](CF_3SO_3)_2$.[38] The metal center has a distorted trigonal bipyramidal, pseudo-$D_{3h}$, coordination

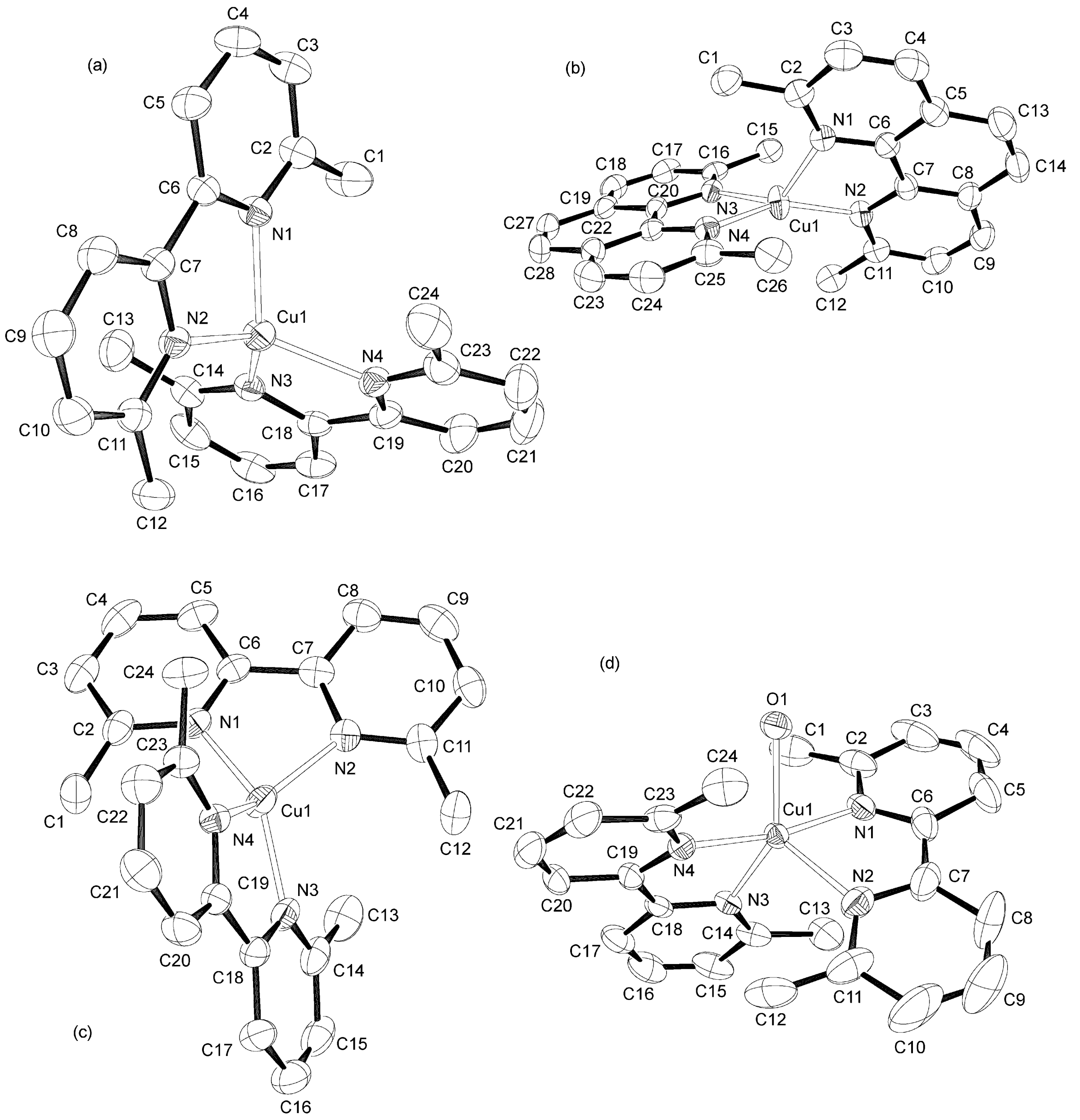

**Fig. 1** ORTEP (50% probability level) of the cationic part of (a) $[Cu(dmbp)_2]ClO_4$, (b) $[Cu(dmp)_2](ClO_4)_2{\cdot}2CH_3NO_2$, (c) $[Cu(dmbp)_2](ClO_4)_2$ and (d) $[Cu(dmbp)_2(H_2O)](ClO_4)_2$. Hydrogen atoms were omitted for clarity.

structure. The two axial positions are occupied by one of the nitrogen donor atoms on each bipyridine ligand. The axial Cu–N distances (1.989(3) and 1.975(3) Å) are somewhat shorter than the bond distances (2.138(3) and 2.057(3) Å for Cu–N and 2.057(3) Å for Cu–O) in the equatorial positions, indicating that the Cu–N bonds at the axial positions are stronger than those at the equatorial positions: such a distortion is expected for the transition metal complexes with vacant d-orbital of the $a_1'$ symmetry in the *Tbp* geometry, while the elongation of the axial bonds is common for compounds of the typical elements in the same structute.[39] The N1–Cu–N2 and N3–Cu–N4 angles are somewhat smaller than the right angle. This distortion is caused by the small bite angle of the didentate dmbp ligand.

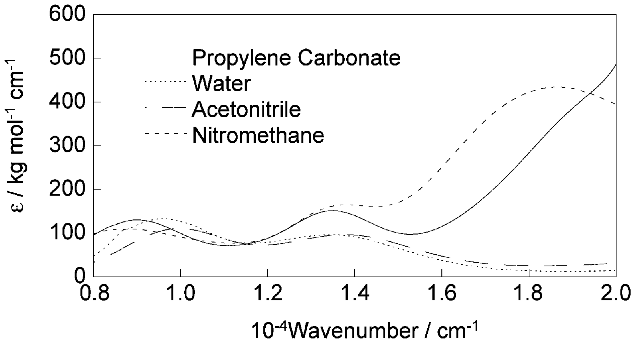

**Fig. 2** Absorption spectra of $[Cu(dmp)_2]^{2+}$ in various solvents.

## Absorption spectra

The UV-Vis absorption spectra of $[Cu(dmp)_2](ClO_4)_2$ in various solvents are shown in Fig. 2. The absorption band maxima in various solvents and those observed in the diffuse reflectance spectrum of the solid sample are summarized in Table 3. In nitromethane and namely propylene carbonate, $[Cu(dmp)_2]^{2+}$ was partly reduced to $[Cu(dmp)_2]^+$ by the residual water in the solvents (*ca.* 1 mmol kg$^{-1}$) within several days and the $[Cu(dmp)_2]^+$ species was recognized by the absorption band at *ca.* 456 nm: it was found that the degree of the reduction of $[Cu(dmp)_2]^{2+}$ in these solvents was proportional to the amount of the residual water in each organic solvent. The molar extinction coefficient of the absorption band at *ca.* 456 nm for $[Cu(dmp)_2]ClO_4$ was *ca.* 5000 kg mol$^{-1}$ cm$^{-1}$ in all solvents:

**Table 2** Selected bond lengths (Å), angles (°) and dihedral angles (°) between the least-squares' planes at 200 K

(a) $[Cu(dmbp)_2]ClO_4$

| | | | |
|---|---|---|---|
| Cu–N1 | 2.047(2) | Cu–N2 | 2.021(2) |
| Cu–N3 | 2.029(2) | Cu–N4 | 2.045(2) |
| N1–Cu–N2 | 81.13(9) | N1–Cu–N3 | 130.42(9) |
| N1–Cu–N4 | 114.02(9) | N2–Cu–N3 | 126.94(9) |
| N2–Cu–N4 | 128.48(9) | N3–Cu–N4 | 81.72(10) |
| Plane [Cu1, N1, N2] *vs.* plane [Cu1, N3, N4] | | | 80.7 |
| Plane of pyridine(1)[a] *vs.* plane of pyridine(2)[b] | | | 2.9(1) |
| Plane of pyridine(3)[c] *vs.* plane of pyridine(4)[d] | | | 13.3(1) |

(b) $[Cu(dmp)_2](ClO_4)_2 \cdot 2CH_3NO_2$

| | | | |
|---|---|---|---|
| Cu–N1 | 1.993(3) | Cu–N2 | 1.982(3) |
| Cu–N3 | 2.054(3) | Cu–N4 | 1.957(3) |
| Cu · · · O6 | 2.485(4) | | |
| N1–Cu–N2 | 83.62(12) | N1–Cu–N3 | 130.00(12) |
| N1–Cu–N4 | 101.02(11) | N2–Cu–N3 | 114.69(11) |
| N2–Cu–N4 | 152.16(13) | N3–Cu–N4 | 83.50(11) |
| O6 · · · Cu–N1 | 131.0(1) | O6 · · · Cu–N2 | 79.2(2) |
| O6 · · · Cu–N3 | 98.8(1) | O6 · · · Cu–N4 | 77.2(2) |
| Plane [Cu1, N1, N2] *vs.* plane [Cu1, N3, N4] | | | 60.34 |
| Plane of bipyridine(12)[e] *vs.* plane of bipyridine(34)[f] | | | 59.45(4) |

(c) $[Cu(dmbp)_2](ClO_4)_2$

| | | | |
|---|---|---|---|
| Cu1–N1 | 2.019(3) | Cu2–N5 | 2.003(3) |
| Cu1–N2 | 1.955(3) | Cu2–N6 | 1.981(3) |
| Cu1–N3 | 2.001(3) | Cu2–N7 | 1.978(3) |
| Cu1–N4 | 1.989(3) | Cu2–N8 | 1.972(3) |
| N1–Cu1–N2 | 83.56(11) | N5–Cu2–N6 | 83.57(12) |
| N1–Cu1–N3 | 133.60(10) | N5–Cu2–N7 | 132.31(11) |
| N1–Cu1–N4 | 115.41(11) | N5–Cu2–N8 | 112.44(11) |
| N2–Cu1–N3 | 103.96(12) | N6–Cu2–N7 | 107.15(11) |
| N2–Cu1–N4 | 146.61(10) | N6–Cu2–N8 | 146.99(10) |
| N3–Cu1–N4 | 83.10(12) | N7–Cu2–N8 | 83.79(11) |
| Plane [Cu1, N1, N2] *vs.* plane [Cu1, N3, N4] | | | 61.40 |
| Plane [Cu2, N5, N6] *vs.* plane [Cu2, N7, N8] | | | 62.78 |
| Plane of bipyridine(12)[g] *vs.* plane of bipyridine(34)[h] | | | 65.16(3) |
| Plane of bipyridine(56)[i] *vs.* plane of bipyridine(78)[j] | | | 68.99(4) |

(d) $[Cu(dmbp)_2(H_2O)](ClO_4)_2$

| | | | |
|---|---|---|---|
| Cu–N1 | 1.989(3) | Cu–N2 | 2.138(3) |
| Cu–N3 | 2.057(3) | Cu–N4 | 1.975(3) |
| Cu–O1 | 2.057(3) | | |
| N1–Cu–N2 | 80.00(15) | N1–Cu–N3 | 104.19(13) |
| N1–Cu–N4 | 169.60(14) | N2–Cu–N3 | 104.02(13) |
| N2–Cu–N4 | 107.42(13) | N3–Cu–N4 | 81.41(13) |
| N1–Cu–O1 | 80.48(12) | N2–Cu–O1 | 117.29(13) |
| N3–Cu–O1 | 138.52(12) | N4–Cu–O1 | 89.52(12) |
| Plane [Cu1, N1, N2] *vs.* plane [Cu1, N3, N4] | | | 80.3 |
| Plane of pyridine(1)[a] *vs.* plane of pyridine(2)[b] | | | 15.0(2) |
| Plane of pyridine(3)[c] *vs.* plane of pyridine(4)[d] | | | 10.2(2) |

[a] Defined by N(1) and C(2)–C(6). [b] Defined by N(2) and C(7)–C(11). [c] Defined by N(3) and C(14)–C(18). [d] Defined by N(4) and C(19)–C(23). [e] Defined by N(1), N(2), C(2)–C(11), C(13) and C(14). [f] Defined by N(3), N(4), C(16)–C(25), C(27) and C(28). [g] Defined by N(1), N(2) and C(2)–C(11). [h] Defined by N(3), N(4) and C(14)–C(23). [i] Defined by N(5), N(6) and C(26)–C(35). [j] Defined by N(7), N(8) and C(38)–C(47).

**Table 3** Absorption band maxima of d–d transitions for $[Cu(dmp)_2](ClO_4)_2$ in various solvents and in the solid state observed by the diffuse reflectance spectrophotometry

| Solvent | Band maximum/cm$^{-1}$ | $\varepsilon$/kg mol$^{-1}$ cm$^{-1}$ |
|---|---|---|
| $H_2O$ | 13432 | 133 |
| | 9588 | 96 |
| MeCN | 13774 | 96 |
| | 9980 | 110 |
| $MeNO_2$ | 20235 | 311 |
| | 17521 | 336 |
| | 13822 | 165 |
| | 8846 | 110 |
| Propylene carbonate | ~ 19300[a] | (420) |
| | 13514 | 151 |
| | 9001 | 130 |
| Solid state | 22169 | — |
| | 18295 | — |
| | 13477 | — |
| | 9183 | — |

[a] Not accurate since the absorption band of Cu(I) which was generated by the decomposition of Cu(II) complex interfered.

this absorption band has been attributed to the metal-to-ligand charge transfer, MLCT.

We failed to record the absorption spectrum of the four-coordinate $[Cu(dmbp)_2]^{2+}$ species, since this complex was very sensitive to moisture. The color of the single crystal was reddish brown, while the powdery sample appeared to be bluish purple. The colors exhibited by this complex are quite different from the deep green color of the previously reported $[Cu(bipy)_2](PF_6)_2$,[37] indicating that the spectral shift depends on the dihedral angle. On the other hand, the reduction of $[Cu(dmp)_2]^{2+}$ in these solvents was minimal and did not affect the rate of reduction reactions (see footnote for "reduction reaction of $[Cu(dmp)_2]^{2+}$ by ferrocene in nitromethane" in this section, and Appendix D).

## Electron self-exchange rate constant for the four-coordinate $[Cu(dmp)_2]^{2+/+}$ couple in nitromethane

$$[Cu(dmp)_2]^{2+} + [^*Cu(dmp)_2]^{+} \xrightarrow{k_{ex}} [Cu(dmp)_2]^{+} + [^*Cu(dmp)_2]^{2+} \qquad (1)$$

The electron self-exchange rate constant, $k_{ex}$, of the $[Cu(dmp)_2]^{2+/+}$ couple was measured by monitoring the broadening of the singlet signal corresponding to the methyl protons on diamagnetic $[Cu(dmp)_2]^+$ with the existence of paramagnetic $[Cu(dmp)_2]^{2+}$. The rate constant, $k_{obs}$, was estimated by using eqn. (2), since no change in the chemical shift of the proton signals was observed for the samples with different concentrations of $[Cu(dmp)_2]^{2+}$: the slow exchange limit was assumed.[40]

$$k_{obs} = \pi(\nu_{obs} - \nu_0) = k_{ex}[Cu(dmp)_2{}^{2+}] \qquad (2)$$

where $\nu_{obs}$ is the full line width of the methyl proton signal at the half maximum height (FWHM) in the presence of $[Cu(dmp)_2]^{2+}$, while $\nu_0$ is the FWHM of the same signal in the absence of $[Cu(dmp)_2]^{2+}$. The dependence of $k_{obs}$ on the concentration of added $[Cu(dmp)_2]^{2+}$ is shown in Fig. 3 (Table S2, ESI†) at various temperatures. The estimated electron self-exchange rate constant at 298.2 K and the activation parameters are listed in Table 4.

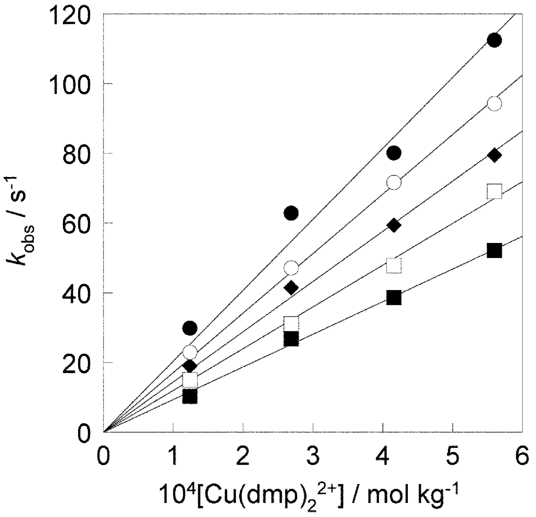

**Fig. 3** Dependence of the first-order rate constant estimated from the broadening of the line width of methyl protons on the concentration of paramagnetic $[Cu(dmp)_2]^{2+}$ in nitromethane. $[Cu(dmp)_2{}^+] = 8.5–9.1 \times 10^{-3}$ mol kg$^{-1}$. $T = 284.4$ K (■), 291.7 K (□), 297.8 K (◆), 307.8 K (○) and 315.7 K (●). Ionic strength was not adjusted in these experiments to avoid possible structural alteration of the Cu(II) species by the ion-pair formation. Concentrations of $[Cu(dmp)_2]^{2+}$ may have up to 10% errors, since reduction of the Cu(II) species by residual water gradually took place during each measurement (it took several days for the completion of measurements after sealing each sample solution in NMR tubes). At higher temperatures than 300 K, the reduction reaction was somewhat faster, and the plots started to scatter.

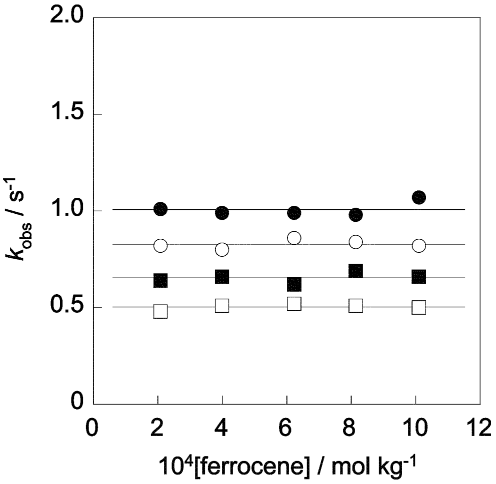

**Fig. 4** Dependence of the rate constant for the reduction reaction of $[Cu(dmp)_2]^{2+}$ by ferrocene on the concentration of ferrocene in nitromethane at various temperatures. $[Cu(dmp)_2]^{2+} = 2.56–4.57 \times 10^{-5}$ mol kg$^{-1}$. $I = 0.1$ mol kg$^{-1}$ (TBAP). $T = 283.2$ K (□), 288.2 K (■), 293.2 K (○) and 298.2 K (●).

## Oxidation reaction of $[Cu(dmp)_2]^+$ by $[Ni(tacn)_2]^{3+}$ in nitromethane

The reaction of $[Cu(dmp)_2]^+$ with $[Ni(tacn)_2]^{3+}$ in nitromethane was first order up to five half-lives and was described by eqn. (3) under the pseudo-first-order conditions of $[Cu(dmp)_2{}^+]_0 \gg [Ni(tacn)_2{}^{3+}]_0$.

$$[Cu(dmp)_2]^+ + [Ni(tacn)_2]^{3+} \xrightarrow{k_{12}} [Cu(dmp)_2]^{2+} + [Ni(tacn)_2]^{2+} \quad (3)$$

$$k_{obs} = k_{12}[Ni(tacn)_2{}^{3+}][Cu(dmp)_2{}^+] \quad (4)$$

Such conditions were chosen because of the instability of $[Ni(tacn)_2]^{3+}$ in nitromethane: $[Ni(tacn)_2]^{3+}$ was slowly reduced during the sample preparation period and the concentration of $[Ni(tacn)_2]^{3+}$ became uncertain when the measurements were carried out. However, a linear dependence of the observed rate constant on the concentration of $[Ni(tacn)_2]^{3+}$ was confirmed by the preliminary experiments in which the pseudo first-order conditions were not fulfilled (Table S3, ESI†): the validity of such treatments have been verified in the previous publication.[41] Therefore, we conclude that the oxidation reaction of $[Cu(dmp)_2]^+$ by $[Ni(tacn)_2]^{3+}$ in nitromethane is described by eqn. (4). The second-order rate constant, $k_{12}$, together with the estimated electron self-exchange rate constant for the $[Cu(dmp)_2]^{2+/+}$ couple at 298.2 K is listed in Table 4. The self-exchange rate constant for the $[Cu(dmp)_2]^{2+/+}$ couple in nitromethane (Table 4) was calculated from the rate constant for the oxidation cross reaction by $[Ni(tacn)_2]^{3+}$, by assuming that the self-exchange rate constant for the $[Ni(tacn)_2]^{3+/2+}$ couple is identical to that observed in acetonitrile (see Appendix F).

This reaction was also examined in the 1 : 1 v/v mixture of acetonitrile and nitromethane, in order to confirm the difference in the reactivity of $[Cu(dmp)_2]^{2+}$ in the $D_2$ symmetry and $[Cu(dmp)_2(acetonitrile)]^{2+}$ in the pseudo-$D_{3h}$ symmetry: the result is also listed in Table 4. It is clear that the electron self-exchange rate constant estimated from the oxidation reaction to produce pseudo-$D_{3h}$-$[Cu(dmp)_2(acetonitrile)]^{2+}$ is smaller than that from the oxidation reaction to produce $D_{2d}$-$[Cu(dmp)_2]^{2+}$ by a factor of 10, indicating that the oxidation reaction of $[Cu(dmp)_2]^+$ by $[Ni(tacn)_2]^{3+}$ proceeds through different pathways when the structure of the product is different.

## Reduction reaction of $[Cu(dmp)_2]^{2+}$ by ferrocene in nitromethane

Experiments were carried out under the conditions of $[ferrocene]_0 \gg [Cu(dmp)_2{}^+]_0$. The kinetic traces were first-order for up to three half-lives.

$$-\frac{d[Cu(II)]}{dt} = k_{obs}[Cu(II)] \quad (5)$$

$$[ferrocene]_0 \gg [Cu(II)]_0 \quad (6)$$

As shown in Fig. 4 (Table S4, ESI†), the rate constant, $k_{obs}$, was small and was not dependent on the concentration of ferrocene within the experimental uncertainty.‡ This is the first completely gated electron transfer reaction among the redox reactions involving simple copper–polypyridine complexes reported to date. The following two-step mechanism that corresponds to path B in Scheme 1 proposed by Rorabacher and co-workers may explain the result in Fig. 4.[8–10]

$$Cu(II) \underset{k_{OQ}}{\overset{k_{OQ}}{\rightleftharpoons}} Cu(II)^* \quad (7)$$

$$Cu(II)^* + A_{red} \xrightarrow{k_{B2}} Cu(I) + A_{ox} \quad (8)$$

where Cu(II), Cu(II)*, $A_{red}$ and $A_{ox}$ represent $[Cu(dmp)_2]^{2+}$ in the ground state, deformed $[Cu(dmp)_2]^{2+}$, ferrocene and ferricenium, respectively. When $k_{B2}[A_{red}] \gg k_{QO}$, the observed first-order rate constant is expressed by eqn. (9).

$$Rate = k_{OQ}[Cu^{II}L] \quad (9)$$

The estimated rate constant, $k_{OQ}$, corresponding to the conformational change in Cu(II) and the activation parameters are listed in Tables 4 and S5, ESI.† This result, together with the results described in the previous section indicates that

---

‡ When water content in nitromethane is more than 10 mmol kg$^{-1}$, $[Cu(dmp)_2]^{2+}$ is reduced within 2–3 h, although when water content in nitromethane is less than *ca.* 0.1 mmol kg$^{-1}$, $[Cu(dmp)_2]^{2+}$ is stable for several days (identified by electrochemical and spectrophotometric methods). Therefore, $[Cu(dmp)_2]^{2+}$ is stable enough for the measurements carried out in this study. In addition, no significant dependence of the rate constants for the reaction between $[Cu(dmp)_2]^{2+}$ and ferrocene on the concentration of residual water was observed for such sample solutions. The results shown in the Table was obtained in the solvent with water content being less than *ca.* 0.1 mmol kg$^{-1}$ (see also Appendix D).

**Table 4** Rate constants (at 25 °C) and activation parameters for the redox reactions involving copper(II)/(I) couples with didentate polypyridine ligands in aqueous, acetonitrile and nitromethane solutions

| Oxidant | Reductant | Solvent | $\log k_{12}$ or $k_{21}$/M$^{-1}$ s$^{-1}$ | $\log k_{11}$/M$^{-1}$ s$^{-1}$ | $\Delta H^*$/kJ mol$^{-1}$ | $\Delta S^*$/J mol$^{-1}$ K$^{-1}$ | Ref. |
|---|---|---|---|---|---|---|---|
| Bis(2,9-dimethyl-1,10-phenanthroline): $Cu^{II/I}(dmp)_2$ | | | | | | | |
| $\mathbf{Cu^{II}L_2{}^{2+/+}}$ | | $H_2O^a$ | | **5.3**[b] | 24 ± 3 | −63 ± 10 | 20[h] |
| $Cu^{II}L_2{}^{2+}$ | Hydroquinones | $H_2O^c$ | pH-Dependent | 5.0 | — | — | 57[i] |
| $Cu^{II}L_2{}^{2+}$ | Hydroquinone | $H_2O^c$ | 7.40 | 4.73 | — | — | 58 |
| $\mathbf{Cu^{II}L_2{}^{2+/+}}$ | | MeCN | | **3.70**[b] | 28 ± 1 | −81 ± 4 | 20[h] |
| $Cu^{II}L_2{}^{2+}$ | $Co^{II}(bpy)_2{}^{2+}$ | MeCN | 2.85[b] | 0.20[b] | 36 ± 2 | −68 ± 6 | 17 |
| $Cu^{II}L_2{}^{2+}$ | $Fe^{II}(Cp)_2$ | MeCN | Gated | $[k_{OQ} = 33]^d$ | 31.5 ± 1.3 | −110 ± 4 | 17 |
| $Cu^{II}L_2{}^{2+}$ | $Fe^{II}(PMCp)_2$ | MeCN | Partly gated | $[k_{OQ} = 34]^d$ | 33.3 ± 0.5 | −104 ± 2 | 17[j] |
| $Ni^{III}(tacn)_2{}^{3+}$ | $Cu^{I}L_2{}^{+}$ | MeCN | 5.43[b] | 3.70[b] | 24 ± 1 | −60 ± 2 | 17 |
| $Mn^{III}(bpyO_2)_3{}^{3+}$ | $Cu^{I}L_2{}^{+}$ | MeCN | 4.46[b] | 4.46[b] | — | — | 17 |
| $Cu^{II}(dmbp)_2{}^{2+}$ | $Cu^{I}L_2{}^{+}$ | MeCN | 4.4 | | 35.5 ± 1.6 | −42 ± 5 | —[e] |
| $\mathbf{Cu^{II}L_2{}^{2+/+}}$ | | $MeNO_2$ | | **5.0**[b] | 15.6 ± 1.3 | −96 ± 4 | —[e,h] |
| $Cu^{II}L_2{}^{2+}$ | $Fe^{II}(Cp)_2$ | $MeNO_2$ | Completely gated | $[k_{OQ} = 1.17]^d$ | 30.7 ± 1.2 | −141 ± 4 | —[e,k] |
| $Ni^{III}(tacn)_2{}^{3+}$ | $Cu^{I}L_2{}^{+}$ | $MeNO_2$ | (~6.5)[b,f] | (~5.3)[b,f,l] | — | — | —[e] |
| $Ni^{III}(tacn)_2{}^{3+}$ | $Cu^{I}L_2{}^{+}$ | Mix[g] | (5.9)[b,f] | (4.3)[b,f,l] | — | — | —[e] |
| $\mathbf{Cu^{II}L_2{}^{2+/+}}$ | | $Me_2CO$ | | **3.48**[b] | 29.2 ± 0.6 | −80 ± 2 | 20[h] |
| Bis(6,6′-dimethyl-2,2′-bipyridyl): $Cu^{II/I}(dmbp)_2$ | | | | | | | |
| $\mathbf{Cu^{II}L_2{}^{2+/+}}$ | | MeCN | | **3.74**[b] | 35.0 ± 0.3 | −56 ± 1 | 55[h] |
| $Cu^{II}L_2{}^{2+}$ | $Ru^{II}(hfac)_3{}^{-}$ | MeCN | 3.77[b] | −0.15[b] | 38 ± 1 | −47 ± 4 | 55 |
| $Cu^{II}L_2{}^{2+}$ | $Co^{II}(bpy)_2{}^{2+}$ | MeCN | 3.28[b] | 0.15[b] | 21.0 ± 0.4 | −112 ± 1 | 55 |
| $Cu^{II}L_2{}^{2+}$ | $Fe^{II}(Cp)_2$ | MeCN | Gated | $[k_{OQ} = 50]^d$ | 30.5 ± 1.3 | −107 ± 1 | 55 |
| $Ru^{III}(hfac)_3$ | $Cu^{I}L_2{}^{+}$ | MeCN | 3.38[b] | −0.7[b] | 41 ± 1 | −38 ± 4 | 55 |
| $Ni^{III}(tacn)_2{}^{3+}$ | $Cu^{I}L_2{}^{+}$ | MeCN | 4.97[b] | 2.83[b] | 24.9 ± 0.5 | −66 ± 2 | 55 |
| $Mn^{III}(bpyO_2)_3{}^{3+}$ | $Cu^{I}L_2{}^{+}$ | MeCN | 3.32[b] | 3.28[b] | 32 ± 1 | −75 ± 4 | 55 |
| Bis(2,9-dimethyl-4,7-diphenyl-1,10-phenanthrolinedisulfonate): $Cu^{II/I}(dpsmp)$ | | | | | | | |
| $\mathbf{Cu^{II}L_2{}^{2+/+}}$ | | $H_2O$ | | **5.7** | — | — | 59[h] |
| $Cu^{II}L_2{}^{2+}$ | Hydroquinone | $H_2O^a$ | 8.15 | 6.4 | — | — | 58 |
| $Cu^{II}L_2{}^{2+}$ | $Fe^{II}(CN)_6{}^{4-}$ | $H_2O$ | Gated | $[k_{OQ} = 229]^d$ | — | — | 43 |
| $Cu^{II}L_2{}^{2+}$ | $Fe^{II}(CN)_6{}^{4-}$ | $H_2O$ | Gated | $[k_{OQ} = 137]^d$ | — | — | 44 |
| $Cu^{II}L_2{}^{2+}$ | $Fe^{II}(EDTA)^{2-}$ | $H_2O$ | Gated | $[k_{OQ} = 139]^d$ | — | — | 44 |
| $Cu^{II}L_2{}^{2+}$ | $Fe^{II}(CN)_5(PPh_3)^{3-}$ | $H_2O$ | Gated | $[k_{OQ} = 130]^d$ | — | — | 44 |
| $Cu^{II}L_2{}^{2+}$ | $Ru^{II}(NH_3)_5pyz^{2+}$ | $H_2O$ | Gated | $[k_{OQ} = 136]^d$ | — | — | 44 |
| $Cu^{II}L_2{}^{2+}$ | $Ru^{II}(NH_3)_5py^{2+}$ | $H_2O$ | 7.2[f] | 1.0 | — | — | 44 |

[a] Chloride ion was used to adjust the ionic strength. [b] Units: kg mol$^{-1}$ s$^{-1}$. [c] Acetate was used to adjust the ionic strength: $I = 0.2$. [d] Units: s$^{-1}$. [e] This work. [f] The reaction was too fast to be measured by the stopped-flow method. [g] 1 : 1 v/v mixture of acetonitrile and nitromethane was used as the solvent. [h] Self-exchange rate constant measured directly by the NMR method. [i] Several parallel reactions. [j] Combined with a high-energy non-adiabatic direct reaction: see text. [k] Only the first-order reaction corresponding to the structural change was observed. [l] Self-exchange rate constant for the $[Ni(tacn)_2]^{3+/2+}$ couple in acetonitrile was used for the calculation of the self-exchange rate constant, $k_{11}$, of the $[Cu(dmp)_2]^{2+/+}$ couple (see Appendix F).

the redox cross reactions involving the $[Cu(dmp)_2]^{2+/+}$ couple proceed through a different pathway from that involving the $[Cu(dmp)_2(solvent)]^{2+}/[Cu(dmp)_2]^{+}$ couple. Reduction reaction of $[Cu(dmp)_2]^{2+}$ with decamethylferrocene in nitromethane was also carried out as a preliminary experiment, in order to examine the influence of the counter reagent on kinetic behavior for the reduction reactions of $[Cu(dmp)_2]^{2+}$ in nitromethane. The reduction reaction of $[Cu(dmp)_2]^{2+}$ with decamethylferrocene also exhibited completely gated behavior with the rate constant of 0.5 ± 0.3 s$^{-1}$ at 25 °C, which is consistent with the rate constant for the structural change observed for the reaction of $[Cu(dmp)_2]^{2+}$ with ferrocene, within the experimental uncertainty.

### Pseudo-electron self-exchange reaction between $[Cu(dmp)_2]^{+}$ and $[Cu(dmbp)_2]^{2+}$ in acetonitrile

The reaction of $[Cu(dmbp)_2]^{2+}$ and $[Cu(dmp)_2]^{+}$ in acetonitrile was first-order for up to five half-lives and was described by eqn. (10) under the pseudo-first-order conditions of $[Cu(dmbp)_2{}^{2+}]_0 \gg [Cu(dmp)_2{}^{+}]_0$.

$$[Cu(dmp)_2]^{+} + [Cu(dmbp)_2]^{2+} \xrightarrow{k_{12}} [Cu(dmp)_2]^{2+} + [Cu(dmbp)_2]^{+} \qquad (10)$$

$$k_{obs} = k_{12}[Cu(dmbp)_2{}^{2+}]_0 \qquad (11)$$

The dependence of the observed rate constant on the concentration of $[Cu(dmbp)_2]^{2+}$ at various temperatures is shown in Fig. 5 (Table S6, ESI†). The second-order rate constant thus estimated at 298.2 K ($I$ = 0.1 mol kg$^{-1}$) is listed in Table 4, together with the activation parameters of the reaction. The observed rate constant, $k_{12}$, may be compared with the self-exchange rate constant for the $[Cu(dmp)_2]^{2+/+}$ couple estimated from the cross reaction in Table 4: the $k_{12}$ value is comparable to that estimated for the self-exchange rate constant observed in the 50% v/v mixture of acetonitrile/nitromethane while the directly measured self-exchange rate constant for the $[Cu(dmp)_2]^{2+/+}$ couple as well as the self-exchange rate constant estimated from the oxidation cross reaction in pure nitromethane were *ca.* 10 times larger than this $k_{12}$.

## Discussion

### Background

Since the discrepancy in the $k_{11}$ values calculated from oxidation and reduction cross reactions was pointed out (detailed explanations are described in Introduction and Appendix A), a number of studies[42–46] including those by Rorabacher and coworkers have been carried out to investigate the gated behaviors exhibited by various Cu(II)/(I) couples.

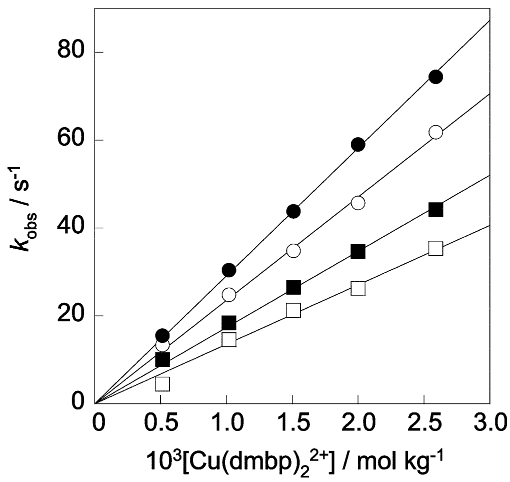

**Fig. 5** Dependence of the rate constant for the oxidation reaction of $[Cu(dmp)_2]^+$ by $[Cu(dmbp)_2]^{2+}$ (the pseudo-exchange reaction) on the concentration of $[Cu(dmbp)_2]^{2+}$ in acetonitrile: $[Cu(dmp)_2{}^+] = 5.0 \times 10^{-5}$ mol kg$^{-1}$. $I = 0.1$ mol kg$^{-1}$ (TBAP). $T = 288.2$ K (□), 293.2 K (■), 298.2 K (○) and 303.2 K (●).

At present, it seems there are two schools of thoughts for explanations of the gated reactions: one attributes the gated phenomena to the sluggish structural change of the coordinated ligands,[8–10] and the other to the non-adiabaticity of the electron transfer reactions involving the ground-state species with the CT-perturbed acceleration of the electron transfer process by means of the conformational change around the Cu center.[17–19] The former explanation, although it seems promising at the first glance, fails to account for the gated reduction reactions of Cu(II)–polypyridine complexes in which no sluggish structural change of the coordinated ligand is required upon geometric changes around the Cu(II) center. On the other hand, the latter explanation seems to lack direct evidence for the non-adiabaticity of the reactions involving Cu(II)/(I) complexes in the ground state although it can account for almost all the gated reactions reported to date.

In this section, we will enforce the latter explanation on the basis of the experimental evidence and on the basis of the perturbation theory for the structural reorganization of metal complexes.

## Structures

The newly synthesized four-coordinate $[Cu(dmp)_2]^{2+}$ species was revealed to be in the $D_2$ symmetry by the X-ray analysis. Therefore, there are two stable conformers for the $[Cu(dmp)_2]^{2+}$ complex: the green five-coordinate $[Cu(dmp)_2(solvent)]^{2+}$ species with a trigonal bipyramidal structure and the reddish-brown four-coordinate $[Cu(dmp)_2]^{2+}$. The latter species is stable in solvents with inferior donor properties such as nitromethane, while the former complex is stabilized in solvents with large donicity: the five-coordinate green species is readily formed by dissolving the four-coordinate complex in acetonitrile (Appendix E).

The absorption spectra of these species in the solid and in solution (Table 3) can be explained on the basis of the selection rules: for a four-coordinate $D_2$ complex, four d–d absorption bands with relatively large molar extinction coefficients are expected, while only three d–d bands corresponding to the transitions to the $b_2$ level from the $e$, $b_1$ and $a_1$ levels are expected for the $D_{2d}$ species. All but the middle band for the complex in the $D_{2d}$ symmetry are allowed to a certain degree for either $x$-, $y$- and/or $z$-polarized light. As for the green complex with a trigonal bipyramidal, pseudo-$D_{3h}$, structure in the solid, only two d–d bands are expected. However, the allowed distortion to the $C_{2v}$ symmetry will split the $e''$ and $e'$ levels, and therefore up to four d–d bands are expected to be observed, depending on the experimental conditions and counter ions[17] (Scheme 2).

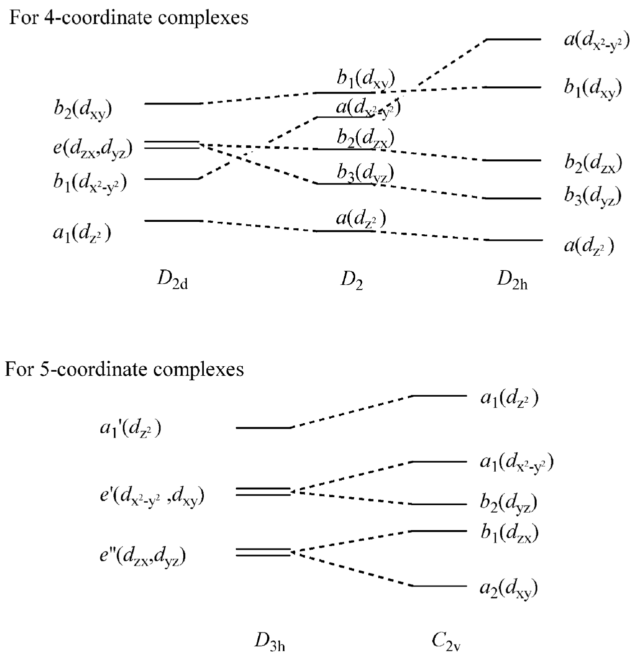

**Scheme 2** Correlation diagrams for different structures of Cu(II)/(I)–polypyridine complexes.

## Examination of the structural change allowed for Cu(I) and Cu(II) complexes on the basis of the Symmetry Rules and the Principle of the Least Motion§

Chemical reactions are considered to proceed through the vibrational activation of molecules, where the term "vibration" includes bond stretches and twist motions allowed for each molecule by the normal coordinate analyses.[24,47] An electronic transition/state mixing is related to the suitable reaction coordinate that is consistent with the corresponding vibrational mode. Therefore, possible activation states and probable products of molecular reactions are predictable on the basis of the Symmetry Rules, which is based on the second-order perturbation theory developed by Jahn and Teller.[34–36] Symmetry Rules require that the possible reaction coordinate should have the same symmetry to that of the "direct product" of the electronic ground state and excited state: the same symmetry as that of the transition density[24] in a sense of the Group Theory. However, most of molecules possess several reaction manifolds possible for reactions, and therefore the applicability of the Symmetry Rules to analyze possible activation modes was considered to be limited. The Principle of the Least Motion (PLM), that states "the lowest activation energy for a reaction is the one that requires the least motion of nuclei and the least disruption of the original electronic configuration,"[25,26] has been successfully coupled with the Symmetry Rules for the prediction of the probable directions of reactions.[24] The correlation diagram of electronic orbitals for each structure is shown in Scheme 2.

**Cu(I) complexes in the $D_{2d}$ symmetry.** Cu(I)–polypyridine complexes are in the $D_{2d}$ symmetry in the ground state. For the complexes that exhibit low-energy MLCT bands, possible low-energy electronic transitions are from the metal $b_2$ or $e$ orbitals to ligand π* orbitals in either of the $a_1$, $b_2$ or $e$ symmetries. These electronic transitions/state mixings correspond to vibration of the $A_1$, $B_2$ and $B_1$ modes: the $A_1$ mode is the totally symmetric vibration, while the $B_2$ and $B_1$ modes lead to the species in the $C_{2v}$ and $D_2$ symmetry, respectively. However, these asymmetric

---

§ When this type of examination is carried out, we may have to consider the symmetry of the whole molecule. However, it has been generally accepted to use "simplified" point group that accounts only for the coordinating atoms around the metal ion for the normal coordinate analyses.[24]

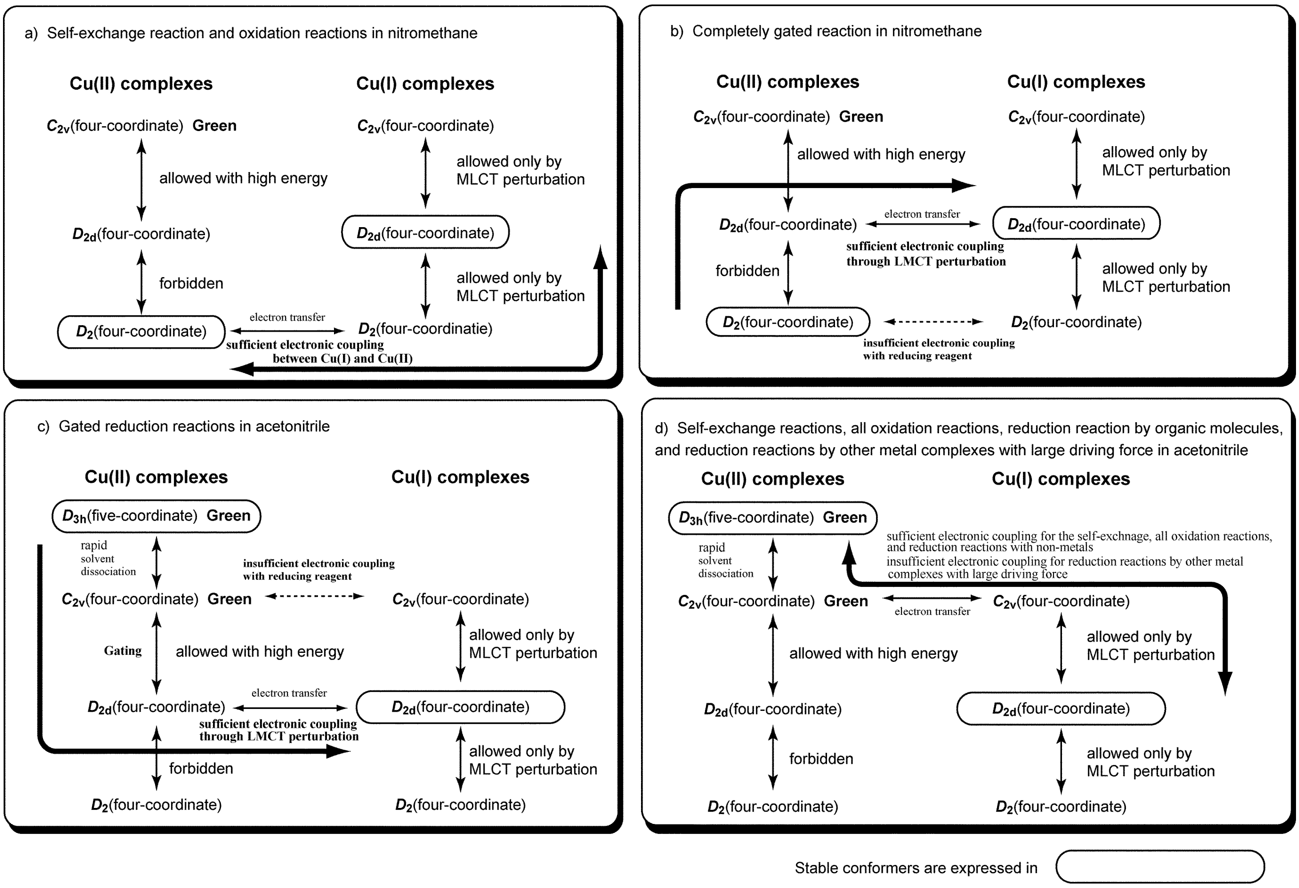

**Scheme 3** The "allowed" and "forbidden" structural changes between possible conformers of four- and five-coordinate Cu(II) and Cu(I) complexes. Observed reaction pathways are shown by the thick arrows.

vibration modes are not induced for the Cu(I) complexes without the low-energy MLCT. Therefore, only Cu(I) complexes in the $D_{2d}$ symmetry that have low-energy MLCT bands are fluxional to exhibit structures among $C_{2v}$, $D_{2d}$ and $D_2$ structures.

**Cu(II) complexes in the $D_{2d}$ and $D_2$ symmetries.** The deformation of the $D_{2d}$ complexes with the $d^9$ electronic configuration to the $D_2$ symmetry requires the $B_1$ mode of vibration. However, the *direct product* for neither the low-energy d–d transitions nor the d–s, s–d and/or d–p, p–d transitions corresponds to this mode, and therefore it is concluded that this deformation from $D_{2d}$ to the $D_2$ structures is forbidden for the Cu(II)–polypyridine complexes on the basis of the Symmetry Rules.¶ On the other hand, consideration on the basis of the combined PLM and Symmetry Rules predicts that the high-energy $a_1$ to $b_2$ electronic transition/state mixing in the $D_{2d}$ complex is coupled with the deformation to the $C_{2v}$ structure, and therefore, this structural inter-conversion is expected to be slow.

**Cu(II) complexes in the pseudo-$D_{3h}$ (*Tbp*) symmetry.** The E′ vibration mode which is related to the low-energy d–d transition/state mixing allows dissociation of the coordinated molecule in the equatorial position. This mode of activation is quite common for transition metal complexes in this symmetry as has been known for *trans*-$[Ni(CN)_2(triphenylphosphine)_3]$.[48] A very rapid ligand substitution reaction has been reported for Cu(II) complexes with the trigonal bipyramid structure.[49–52] On the other hand, the structural change between $C_{2v}$ and $D_{2d}$ structures is a high-energy process as described above. In conclusion, the dissociation of a coordinated solvent molecule from $[Cu(dmp\ or\ dmbp)_2(solvent)]^{2+}$ in the pseudo-$D_{3h}$ symmetry readily occurs to produce the $[Cu(dmp\ or\ dmbp)_2]^{2+}$ species in the $C_{2v}$ symmetry, while further deformation of this species to the one in the $D_{2d}$ symmetry is a high-energy process that should be rather slow. In Scheme 3, summarized are the "allowed" and "forbidden" structural changes between the possible conformers of four- and five-coordinate Cu(II) and Cu(I) complexes.

## Electron transfer reactions involving $[Cu(dmp)_2]^{2+/+}$ (Scheme 3)

In the case of electron self-exchange reaction of the $[Cu(dmp)_2]^{2+/+}$ couple in nitromethane, the ground-state structures in the solid are retained: the Cu(I) complex is in the $D_{2d}$ symmetry and the Cu(II) complex in the $D_2$ symmetry. The symmetry argument given above concludes that the change between the $D_{2d}$ and $D_2$ structures is forbidden for Cu(II), while it is allowed for Cu(I) species that exhibit low-energy MLCT bands. Therefore, the direct electron self-exchange reaction in nitromethane should involve major deformation of only Cu(I) from the ground-state $D_{2d}$ to the excited $D_2$ structure (Scheme 3(a)). Since this structural change proceeds smoothly along the single reaction coordinate (allowed), the reaction is not gated: the electron self-exchange reaction between the four-coordinate $[Cu(dmp)_2]^{2+/+}$ complexes takes place in a concerted manner and rapid as seen in Table 4, although the inner-sphere structural reorganization may be uneven for the Cu(I) and Cu(II) species (symmetric bond stretching modes of Cu(II) and Cu(I) also contribute to the overall activation barrier).

The oxidation reaction of $[Cu(dmp)_2]^+$ by $[Ni(tacn)_2]^{3+}$ in nitromethane takes place through the same route: the MLCT induces the change from the $D_{2d}$ to $D_2$ structure for Cu(I) and this transition also causes the delocalization of the d electrons over the ligands' π* level so as to let the CT-perturbed ET possible[19]

---

¶ We examined the direct product of the reverse reaction of the conformational change from $D_{2d}$ to $D_2$ for the examination of the reaction modes, since we cannot easily deal with the normal vibration modes for the $D_2$ point group. We relied on the Principle of Microscopic Reversibility.

(see later discussion). This activation process is inevitable since only this route leads to the stable product in nitromethane, $[Cu(dmp)_2]^{2+}$ in the $D_2$ symmetry (Scheme 3(a)).

On the other hand, the reduction reaction of $[Cu(dmp)_2]^{2+}$ in the $D_2$ symmetry by ferrocene should be sluggish, since no smooth single reaction coordinate (concerted process) that leads to stable Cu(I) in the $D_{2d}$ structure exists for this reaction, according to the Symmetry Rules and PLM. Therefore, the reaction has to proceed through either of the following two high-energy processes: (1) *via* the inner-sphere reorganization of Cu(II) through the very high-energy path without bond rupture between Cu(II) and N or through the dissociation of one of the bonds between Cu(II) and N, or (2) *via* the product excited state, $D_2$-Cu(I).[53,54] The structural rearrangements in (1) take place prior to the formation of the encounter complex, because these rearrangements are high-energy activation processes which are not allowed to occur within the encounter complex, according to the discussion by Brunschwig and Sutin.[53] When the rate constant for the reverse reaction of structural change, $k_{QO}$, is very small compared with the succeeding electron transfer process, the overall rate constant is independent of the concentration of the counter reagent as observed in this study. To the contrary, the observed rate constant should depend on the concentration of the counter reagent when the reaction proceeds through (2). Therefore, it is concluded that the reduction reaction of $D_2$-Cu(II) by ferrocene proceeds through (1) (Scheme 3(b)). The activation parameters for this reaction, $\Delta H^* = 30.7$ kJ mol$^{-1}$ and $\Delta S^* = -141$ J mol$^{-1}$ K$^{-1}$, may indicate that the inner-sphere reorganization in (1) takes place without bond dissociation between Cu(II) and N: a very high-energy twist to form $D_{2d}$-Cu(II) may occur, although this process is symmetry-forbidden and is expected to be non-adiabatic (crossing occurs at the intersection of the two states with different symmetries).[54] The completely gated phenomenon observed for the reduction of Cu(II) in the $D_2$ symmetry indicates that the process corresponding to $k_{QO}$ is either non-adiabatic or requires very high activation energy (Appendix G). The experimental results tell us that the pathway (2) requires higher energy than pathway (1), the reason of which may be given by considering the extremely low energy level of the d-orbitals in the Cu(II) species (see below): a CT perturbation in the Cu(II) complexes seems to be essential for the sufficient overlap between the donor and acceptor orbitals to ensure rapid ET for the cross reactions with other metal complexes. It was shown in this study that the Cu(II) complex in the $D_2$ symmetry does not exhibit low-energy LMCT, while Cu(II) in the $D_{2d}$ symmetry certainly exhibits low-energy LMCT band, as described in the previous article.[19]

The experimental result for the pseudo electron self-exchange reaction between $[Cu(dmbp)]^{2+}$ and $[Cu(dmp)_2]^{+}$ in acetonitrile (Table 4) indicates that the electron transfer between Cu(II) in the trigonal bipyramidal (pseudo-$D_{3h}$) structure and Cu(I) in the $D_{2d}$ symmetry is fast: the pseudo exchange rate constant (*ca.* $10^4$ kg mol$^{-1}$ s$^{-1}$) is as large as the self-exchange rate constant for each redox couple measured directly by the NMR method. On the other hand, all of the reported cross reduction reactions of these Cu(II) species by other metal complexes were gated and the estimated self-exchange rate constants for these Cu(II)/(I) couples by using the Marcus cross relation are much smaller than $10^4$ kg mol$^{-1}$ s$^{-1}$.[17,55] These observations strongly indicate that the "reaction mode" is different for the reactions between Cu(II) and Cu(I) complexes from that between Cu(II) and other metal centers: *the gated electron transfer is induced only for the cross reactions of Cu(II) species with other metal complexes* (Table 4). Most interestingly, the outer-sphere reduction reactions of Cu(II) by hydorquinones are very rapid, and the calculated self-exchange rate constant for the Cu(II)/(I) couples are as large as $10^5$ dm$^3$ mol$^{-1}$ s$^{-1}$ (Table 4): it seems that the electronic coupling between the d-orbital (SOMO) of Cu(II) and the HOMO levels of hydroquinones are sufficiently large, while the electronic coupling between the d-orbital (SOMO) of Cu(II) and the d-orbital (HOMO/SOMO) of other metal complexes, such as $[Ni(tacn)_2]^{3+}$ and $[Ru(hfac)_3]^{+/0}$, is rather small. The very low HOMO and SOMO energy levels in the Cu(I) and Cu(II) complexes are evidenced also by the very large ionization potentials of the copper element: the second ionization potential of Cu is 20.29 eV while the third ionization potential is as high as 36.84 eV,[56] which are some 2 eV larger than those for other metals. It seems that the very low d-electron energy levels in Cu(II)/(I) complexes originate from the very large effective nuclear charge of central Cu, and cause insufficient coupling with the d-orbitals of other metal complexes for the outer-sphere electron transfer reactions.

Symmetry Rules and the PLM indicate that the dissociation of the solvent molecule from the trigonal plane of $[Cu(dmp)_2(solvent)]^{2+}$ is allowed to form four-coordinate $[Cu(dmp)_2]^{2+}$ in the $C_{2v}$ symmetry, while the structural change of this species further to $[Cu(dmp)_2]^{2+}$ in the $D_{2d}$ symmetry requires high-energy electronic transitions/state mixing. Therefore, the reaction is gated when the inner-sphere activation of Cu(II) species occurs along this process, *Tbp* (pseudo-$D_{3h}$) → $C_{2v}$ → $D_{2d}$. (Scheme 3(c))

In the electron self-exchange reactions, the $C_{2v}$ complex produced by the allowed rapid dissociation of a solvent molecule from the trigonal plane of the *Tbp* complex may directly react with $[Cu(dmp)_2]^{+}$ in the same structure, since the structural change from $D_{2d}$-Cu(I) to the $C_{2v}$ geometry through the $B_2$ vibration mode is allowed by the MLCT perturbation according to the Symmetry Rules and PLM. Therefore, the direct self-exchange reaction between green Cu(II) (*Tbp*) and red Cu(I) ($D_{2d}$), appears concerted through the common activation state with the $C_{2v}$ structure (Scheme 3(d)) for both Cu(I) and Cu(II) species, since sufficient electronic coupling is achieved between the Cu(I) and Cu(II) complexes with like structures. The evidence for the "concertedness" of the electron self-exchange reaction has been given by the volume analyses for the self-exchange reaction of the $[Cu(dmp)_2]^{2+/+}$ couple in acetonitrile.[20] However, this mode of reaction is not favored in the cases of the cross reduction reactions by metal complexes other than Cu and cannot compete with the gated pathway through *Tbp* (pseudo-$D_{3h}$) → $C_{2v}$ → $D_{2d}$, since a sufficient electronic coupling between the $C_{2v}$-Cu(II) and the counter reagent cannot be achieved through this process: the reaction of $D_{2d}$-Cu(II) with metal complexes other than Cu are rapid (but gated) since only $D_{2d}$-Cu(II) exhibits the LMCT-perturbed enhancement of the electronic coupling with the counter reagents (Scheme 3(d)).

The experimental results and the symmetry argument indicate that the electron self-exchange reactions between copper complexes are not gated but concerted. This also explains why the self-exchange reactions for most of the macrocyclic polythioether complexes reported by Rorabacher and co-workers are also fast (and probably concerted) while the oxidation cross reactions of these complexes are gated: the Cu(II) complexes with polythioether ligands exhibit strong LMCT bands while corresponding Cu(I) complexes are colorless. Relatively low HOMO and SOMO energy levels in the Cu(I) and Cu(II) complexes are responsible for the non-adiabaticity of the electron transfer reactions with other metal complexes: the reduction reaction of $[Cu(dmp)_2(solvent)]^{2+}$ complex have been reported to be rapid with compounds of typical elements, such as hydroquinones, with which the electronic coupling seems sufficient for the adiabatic ET to occur.[57,58]

As a result, we may derive the following conclusions: (1) it is essential for the occurrence of the gated behavior that either structural changes expected for the concerted process is forbidden by the Symmetry Rules or the reaction through the free energy surface of the concerted process is non-adiabatic, (2) structural change of the ground-state species occurs so as to maximize the electronic coupling between the reactants through the CT-perturbation, (3) structural change in the gated process can be explained on the basis of the Symmetry Rules and PLM, and (4) the high-energy structural changes lead to the ordinary gated behavior while structural changes through the symmetry-forbidden processes lead to the completely gated reaction (since back reaction of this structural change is also forbidden by the principle of microscopic reversibility). These conclusions can explain the mysteriously small self-exchange rate constants estimated for the $[Cu(dmbp)_2]^{2+/+}$ couple from the oxidation and reduction cross reactions by $[Ru(hfac)_3]^{-/0}$ in acetonitrile[18] (note that the electron self-exchange rate constant measured directly by the NMR method is *ca.* $10^4$ kg mol$^{-1}$ s$^{-1}$ and rapid, see Appendix B). From the principle of microscopic reversibility, it is certain that both oxidation and reduction reactions should proceed through the identical pathway with the lowest possible activation energy. The four factors given above indicate that the oxidation/reduction reactions of $[Cu(dmbp)_2(acetonitrile)]^{2+}/[Cu(dmbp)_2]^+$ with $[Ru(hfac)_3]^{0/-}$ should either be gated or proceed along the non-adiabatic free-energy surface. The small self-exchange rate constant estimated from the oxidation direction indicates that the electronic coupling between Cu(I) and Ru(III) complexes is small and both oxidation and reduction reactions proceed through the non-adiabatic process. The fact that the estimated self-exchange rate constant (0.7 kg mol$^{-1}$ s$^{-1}$) for the reactions of $[Cu(dmbp)_2]^{2+/+}$ with $[Ru(hfac)_3]^{0/-}$ is comparable to the apparent self-exchange rate constants for the evidently gated reduction reactions of $[Cu(dmp)_2]^{2+}$ in acetonitrile (1.6 kg mol$^{-1}$ s$^{-1}$)[17] indicates that the apparent free energy barrier for the non-adiabatic reactions of $[Cu(dmbp)_2]^{2+/+}$ and $[Ru(hfac)_3]^{0/-}$ is not significantly different from that for the gated reduction reactions of $[Cu(dmbp)_2]^{2+}$ in acetonitrile.

## Appendix A

The use of the term "gated" was referred to, by Hoffman and Ratner,[60] the specific situation in which conformational change (or similar slow kinetic phenomenon) of one reactant becomes rate controlling and the reaction becomes truly first-order. However, the usage of this term became diverted to the reactions in which a large conformational change precedes the electron transfer (ET) process, since the original definition of the gated ET is taken to be the extreme case where the first-order rate constant of the back reaction for the conformational change, $k_{QO}$, is very small compared with the product of the rate constant for the ET process, $k_{ET}$, and the concentration of the reagent of the cross reaction, $k_{QO} \ll k_{ET}$[Reducing reagent]. Unfortunately, there have been very few cases in which a truly first-order reaction was observed: the reduction reaction of $[Cu(dmp)_2]^{2+}$ by ferrocene in nitromethane reported in this study is one of such a rare example. We, therefore, decided to use the term "gated" for the general cases where the reaction takes place in two steps with the sluggish conformational change before the ET process, and the term "Completely gated" was used for the reaction in which the observed rate constant was actually first-order (independent of the concentration of the reducing reagent), to refer to the original definition by Hoffman and Ratner, in this article.

## Appendix B

The redox potentials for the $[Cu(dmbp)_2]^{2+/+}$ and $[Ru(hfac)_3]^{0/-}$ couples are similar to each other in acetonitrile, and we were able to examine both oxidation reaction of $[Cu(dmbp)_2]^+$ by $[Ru(hfac)_3]$ and reduction reaction of $[Cu(dmbp)_2]^{2+}$ by $[Ru(hfac)_3]^-$ in acetonitrile by altering the experimental conditions.[18] Although the oxidation reactions of $[Cu(dmbp)_2]^+$ by other metal complexes have never been gated in acetonitrile, including the self-exchange reaction and the pseudo-exchange reaction with $[Cu(dmp)_2]^{2+}$, the self-exchange rate constant estimated from the oxidation reaction of $[Cu(dmbp)_2]^+$ by $[Ru(hfac)_3]^0$ was as small as that estimated from the reduction reaction of $[Cu(dmbp)_2]^{2+}$ by $[Ru(hfac)_3]^-$. As for the reactions of $[Cu(dmbp)_2]^{2+/+}$ with $[Ru(hfac)_3]^{0/-}$, the reactions in both directions should undergo through the identical free-energy surface. A similar argument was also given by Stanbury *et al.* in their recent paper for the reactions with Cu-bite complexes.[61] The dependence of the rate constants for the reduction reactions with $[Ru(hfac)_3]^-$ on the concentration of $[Ru(hfac)_3]^-$ was not saturating but was linear. Although we may tend to say, "both directions are gated," it is not true according to the square scheme. We deduced that both oxidation and reduction reactions are non-adiabatic. If the reduction reaction is gated, the following ET process should be rapid. In such a case, the reverse reaction, the oxidation reaction, should proceed through the product excited state and rapid according to the theory by Brunschwig and Sutin.[53,54]

## Appendix C

Recent publication by Garner and co-workers[62] seems to verify our proposal: a four-coordinate Cu(II)/(I) couple with imidazole ligands did not exhibit gated behavior. It appears that the redox reactions of Cu(II)/(I) couples with low-energy LM- and MLCT bands proceed through the ordinary concerted mechanism, since the LM- and MLCT-perturbed superexchange or sequential ET is induced for the cross reactions involving such couples.

## Appendix D

Under the experimental conditions, observation of the cyclic voltammogram confirmed that the CV of $[Cu(dmp)_2]^{2+}$ solution was identical to that for the solution of $[Cu(dmp)_2]^+$ with identical concentration, for more than several hours. The ratio of the anodic and cathodic currents was always 1 : 1 and no significant shift of the redox potential was observed within the experimental uncertainty (decomposition of the Cu(II) complex was not observed under the experimental conditions).

When excess dmp was added to the nitromethane solution, reduction of $[Cu(dmp)_2]^{2+}$ became significant (it took only *ca.* 1 min. to have all Cu(II) species in the solution reduced to $[Cu(dmp)_2]^+$ when *ca.* 10 mmol kg$^{-1}$ of free dmp existed in the solution). Since addition of free ligand introduces small amount of water, it seems that the existence of water certainly accelerate the reduction reaction. However, it should also be noted that the reduction product was identified as the $[Cu(dmp)_2]^+$ complex by the spectrophotometric and electrochemical analyses, in these experiments. Although it seems that water molecule acted as the base, we did not make any effort to identify the reaction products, since the degree of the reduction was not significant under the experimental conditions used in this study (typical value of less than 0.1% for the reduction was estimated from the electrochemical analyses). Therefore, $[Cu(dmp)_2]^{2+}$ is stable in nitromethane (and in acetonitrile). A similar result was reported for another Cu(II) complex in acetone by Swaddle and co-workers[63]: although a rapid ligand exchange reaction was observed by the addition of the didentate free ligand to the solution of Cu(II) complex, no release of the coordinated ligand was observed without addition of free ligand. Therefore, all of the experimental evidence confirms that (1) $[Cu(dmp)_2]^{2+}$ is stable in nitromethane and (2) the structure was certainly retained in solution as identified by the spectrophotometric and electrochemical methods.

## Appendix E

By the molecular mechanics calculations using a Cache program (MM3), the formation energies of Cu(II)–dmp complexes were 54.60, 111.55 and 150.14 kcal mol$^{-1}$ for *Tbp* ($D_{3h}$) with water, $D_2$ and $D_{2d}$ complexes, respectively. These results indicate that the *Tbp* complex is stable in solvents that have large donicity, while $D_2$ conformer is more stable than the $D_{2d}$ conformer in poor donor solvents such as nitromethane. These results are consistent with the experimental observations: the structure of the $D_2$ complex is certainly retained in nitromethane and it converts to the *Tbp* structure in acetonitrile, although the fast exchange of the coordinated solvent molecule takes place in acetonitrile, as expected from the Symmetry Rules.

### Appendix F

According to the Marcus' theory,[14–16] the self-exchange rate constant for a redox couple depends essentially on the high- and low-frequency dielectric constants of the solvent. Since these parameters are similar to each other for nitromethane and acetonitrile, the self-exchange rate constant for the [Ni(tacn)$_2$]$^{3+/2+}$ couple in acetonitrile was used for the calculations of the self-exchange rate constants for the [Cu(dmp)$_2$]$^{2+/+}$ couple in nitromethane and 1 : 1 v/v mixture of nitromethane and acetonitrile.

### Appendix G

As for the reactions of four-coordinate Cu(II)/(I) couple, Stanbury and co-workers reported a completely gated self-exchange reaction by the NMR study.[61] Authors suggested that the ET is accelerated by the intervention of the inner-sphere mechanism. We agree with this idea since we believe that the acceleration of the ET rate by the inner-sphere mechanism should be treated as either of the superexchange or sequential transfer in a sense of quantum mechanics.[19] Very different structures of these species ($T_d$ and $D_{4h}$) seem to be the reason since it requires forbidden structural inter-conversion ($D_{4h}$–$T_d$). Therefore, it seems both directions are regulated by the sluggish geometric changes in Cu(I) as well as Cu(II). Moreover, the reduction/oxidation reactions by Ru(III)/(II) couples with Cu(II)/(I)-bite complexes are similar to those observed for the reactions with Cu(II)/(I)-dmbp couples in our previous study:[18] the reactions have to be treated on the basis of the microscopic reversibility. The self-exchange rate constants estimated from both directions are identical to each other within the experimental uncertainty, as indicated in their study. On the other hand, results for the cross reactions have been published later by the same authors:[64] although both oxidation and reduction directions seems to be gated in the cross reactions, the reported rate constants for the estimated self-exchange reaction was too small to explain the observed line broadening of the NMR signals for the self-exchange study of the same couple. If we trust the results for the cross reactions, it seems both oxidation and reduction directions are gated. Such sluggish conformational changes may be attributed to the large energy barrier necessary for the twist of the macrocyclic ligands. Since an inversion around a carbon center requires *ca.* 30–40 kJ mol$^{-1}$ of activation energy, the reaction of Cu(II)/(I) couples with macrocyclic ligands may also be regulated by the distortion within the ligand. The discussions given in this article do not account for such distortions, and the authors of the present article admit that the explanation by Rorabacher and co-workers are valid for *most* reactions involving Cu(II)/(I) couples with macrocyclic polythioether ligands.

## References

1 R. P. J. Williams, *Eur. J. Biochem.*, 1995, **234**, 363–381.
2 W. Kaim and B. Schwederski, in *Bioinorganic Chemistry: Inorganic Elements in the Chemistry of Life*, Wiley, Chichester, 1994.
3 B. L. Vallee and R. J. P. Williams, *Proc. Natl. Acad. Sci. USA*, 1968, **59**, 498–505.
4 M. A. Augustin and J. K. Yandell, *J. Chem. Soc., Chem. Commun.*, 1978, 370–372.
5 M. A. Augustin and J. K. Yandell, *Inorg. Chem.*, 1979, **18**, 577–583.
6 J. K. Yandell, in *Copper Coordination Chemistry, Biochemical and Inorganic Perspectives*, ed. K. D. Karlin and J. Zubieta, Adenine Press, New York, 1983, pp. 157, and references therein.
7 C.-W. Lee and F. C. Anson, *J. Phys. Chem.*, 1983, **87**, 3360–3362.
8 M. J. Martin, J. F. Endicott, L. A. Ochrymowycz and D. B. Rorabacher, *Inorg. Chem.*, 1987, **26**, 3012–3022.
9 N. E. Meager, K. L. Juntunen, M. J. Heeg, C. A. Salhi, L. A. Ochrymowycz and D. B. Rorabacher, *J. Am. Chem. Soc.*, 1992, **114**, 10411–10420.
10 D. B. Rorabacher, N. E. Meagher, K. L. Juntunen, P. V. Robandt, G. H. Leggett, C. A. Salhi, B. C. Dunn, R. R. Schroeder and L. A. Ochrymowycz, *Pure Appl. Chem.*, 1993, **65**, 573–578.
11 P. V. Robandt, R. R. Schroeder and D. B. Rorabacher, *Inorg. Chem.*, 1993, **32**, 3957–3963.
12 C. A. Salhi, Q. Yu, M. J. Heeg, N. M. Villeneuve, K. L. Juntunen, R. R. Schroeder, L. A. Ochrymowycz and D. B. Rorabacher, *Inorg. Chem.*, 1995, **34**, 6053–6064.
13 D. B. Rorabacher, *Chem. Rev.*, 2004, **104**, 651–697.
14 R. D. Cannon, in *Electron Transfer Reactions*, Butterworth, London, 1980.
15 N. Sutin, *Prog. Inorg. Chem.*, 1983, **30**, 441–498.
16 R. B. Jordan, in *Reaction Mechanisms of Inorganic and Organometallic Systems*, Oxford University Press, New York, 2nd edn., 1998.
17 N. Koshino, Y. Kuchiyama, H. Ozaki, S. Funahashi and H. D. Takagi, *Inorg. Chem.*, 1999, **38**, 3352–3360.
18 N. Koshino, Y. Kuchiyama, S. Funahashi and H. D. Takagi, *Chem. Phys. Lett.*, 1999, **306**, 291–296.
19 S. Itoh, S. Funahashi, N. Koshino and H. D. Takagi, *Inorg. Chim. Acta*, 2001, **324**, 252–265.
20 H. Doine (Takagi), Y. Yano and T. W. Swaddle, *Inorg. Chem.*, 1989, **28**, 2319–2322.
21 S. Itoh, S. Funahashi and H. D. Takagi, *Chem. Phys. Lett.*, 2001, **344**, 441–449.
22 H. Yokoi and A. W. addison, *Inorg. Chem.*, 1977, **16**, 1341–1349.
23 Y. Kuchiyama, N. Kobayashi and H. D. Takagi, *Inorg. Chim. Acta*, 1998, **277**, 31–36.
24 R. G. Pearson, in *Symmetry Rules for Chemical Reactions*, Wiley, New York, 1976.
25 F. O. Rice and E. Teller, *J. Chem. Phys.*, 1938, **6**, 489–496.
26 F. O. Rice and E. Teller, *J. Chem. Phys.*, 1939, **7**, 199.
27 A. McAuley, P. R. Norman and O. Olubuyide, *Inorg. Chem.*, 1984, **23**, 1938–1943.
28 A. Altomare, M. C. Burla, M. Camalli, M. Cascarono, C. Giacovazzo, A. Guagliardi and G. Polidori, *J. Appl. Crystallogr.*, 1994, **27**, 435.
29 G. M. Sheldrick, *SHELXL97*, University of Göttingen, Germany, 1997.
30 Molecular Structure Corporation and Rigaku Co. Ltd., TeXsan, Single crystal structure analysis software, ver. 1.11, The Woodlands, TX, USA and Akishima, Tokyo, Japan, 2000.
31 P. J. Burke, D. R. McMillin and W. R. Robinson, *Inorg. Chem.*, 1980, **19**, 1211–1214.
32 M. Munakata, S. Kitagawa, A. Asahara and H. Masuda, *Bull. Chem. Soc. Jpn.*, 1987, **60**, 1927–1929.
33 B. W. Skelton, A. F. Waters and A. H. White, *Aust. J. Chem.*, 1991, **44**, 1207–1215.
34 H. A. Jahn and E. Teller, *Proc. R. Soc. London, Ser. A*, 1937, **161**, 220–235.
35 H. A. Jahn, *Proc. R. Soc. London, Ser. A*, 1938, **164**, 117–131.
36 U. Öpik and M. H. L. Pryce, *Proc. R. Soc. London, Ser. A*, 1957, **238**, 425–447.
37 J. Foley, S. Tyagi and B. J. Hathaway, *J. Chem. Soc., Dalton Trans.*, 1984, 1–5.
38 D. Tran, B. W. Skelton, A. H. White, L. E. Laverman and P. C. Ford, *Inorg. Chem.*, 1998, **37**, 2505–2511.
39 K. Mislow, *Acc. Chem. Res.*, 1970, **3**, 321–331.
40 S. F. Lincoln, *Prog. React. Kinet.*, 1977, **9**, 1–91.
41 S. Itoh, M. Katsuki, T. Noda, K. Ishihara, M. Inamo and H. D. Takagi, *Dalton. Trans.*, 2004, 1862–1866.
42 C.-W. Lee and F. C. Anson, *Inorg. Chem.*, 1984, **23**, 837–844.
43 N. Al-Shatti, A. G. Lappin and A. G. Sykes, *Inorg. Chem.*, 1981, **20**, 1466–1469.
44 P. Leupin, N. Al-Shatti and A. G. Sykes, *J. Chem. Soc., Dalton Trans.*, 1982, 927–930.
45 A. E. Allan, A. G. Lappin and M. C. M. Laranjeira, *Inorg. Chem.*, 1984, **23**, 477–482.
46 B. Xie, T. Elder, L. J. Wilson and D. M. Stanbury, *Inorg. Chem.*, 1999, **38**, 12–19.
47 B. E. Douglas and C. A. Hollingsworth, in *Symmetry in Bonding and Spectra*, Academic Press, New York, 1985.
48 C. G. Grimes and R. G. Pearson, *Inorg. Chem.*, 1974, **13**, 970–977.
49 D. P. Rablen, H. W. Dodgen and J. P. Hunt, *J. Am. Chem. Soc.*, 1972, **94**, 1771.
50 R. J. West and S. F. Lincoln, *J. Chem. Soc., Dalton Trans.*, 1974, 281–284.
51 D. H. Powell, A. E. Merbach, I. Fábián, S. Schindler and R. van Eldik, *Inorg. Chem.*, 1994, **33**, 4468–4473.

52 S. F. Lincoln, J. H. Coates, B. G. Doddridge, A. M. Hounslow and D. L. Pisaniello, *Inorg. Chem.*, 1983, **22**, 2869–2872.
53 B. S. Brunschwig and N. Sutin, *J. Am. Chem. Soc.*, 1989, **111**, 7454–7465.
54 N. Sutin and B. S. Brunschwig, in Mechanistic Aspects of Inorganic Reactions, ed. D. B. Rorabacher and J. F. Endicott, *ACS Symposium Series No. 198*, American Chemical Society, Washington DC, 1982, pp. 105.
55 N. Koshino, Y. Kuchiyama, S. Funahashi and H. D. Takagi, *Can. J. Chem.*, 1999, **77**, 1498–1507.
56 D. F. Shriver and P. W. Atkins, in *Inorganic Chemistry*, Oxford University Press, Oxford, 3rd edn., 1999.
57 J. D. Clemmer, G. K. Hogaboom and R. A. Holwerda, *Inorg. Chem.*, 1979, **18**, 2567–2572.
58 R. A. Holwerda, *Inorg. Chem.*, 1982, **21**, 2107–2109.
59 K. L. Juntunen, PhD Thesis, Wayne State University, 1992.
60 B. M. Hoffman and M. A. Ratner, *J. Am. Chem. Soc.*, 1987, **109**, 6237–6243.
61 S. Flanagan, J. Dong, K. Haller, S. Wang, W. R. Scheidt, R. A. Scott, T. R. Webb, D. M. Stanbury and L. J. Wilson, *J. Am. Chem. Soc.*, 1997, **119**, 8857–8868.
62 J. McMaster, R. L. Beddoes, D. Collison, D. R. Eardley, M. Helliwell and C. D. Garner, *Chem. Eur. J.*, 1996, **2**, 685–693.
63 P. D. Metelski, A. S. Hinman, H. D. Takagi and T. W. Swaddle, *Can. J. Chem.*, 1995, **73**, 61–69.
64 B. Xie, L. J. Wilson and D. M. Stanbury, *Inorg. Chem.*, 2001, **40**, 3606–3614.